World Academy of Science, Engineering and Technology
International Journal of Biomedical and Biological Engineering
Vol:3, No:6, 2009

Modeling of Pulsatile Blood flow in a weak magnetic field

Chee Teck Phua, Gaëlle Lissorgues

***Abstract*—** Blood pulse is an important human physiological signal commonly used for the understanding of the individual physical health. Current methods of non-invasive blood pulse sensing require direct contact or access to the human skin. As such, the performances of these devices tend to vary with time and are subjective to human body fluids (e.g. blood, perspiration and skin-oil) and environmental contaminants (e.g. mud, water, etc). This paper proposes a simulation model for the novel method of non-invasive acquisition of blood pulse using the disturbance created by blood flowing through a localized magnetic field. The simulation model geometry represents a blood vessel, a permanent magnet, a magnetic sensor, surrounding tissues and air in 2-dimensional. In this model, the velocity and pressure fields in the blood stream are described based on Navier-Stroke equations and the walls of the blood vessel are assumed to have no-slip condition. The blood assumes a parabolic profile considering a laminar flow for blood in major artery near the skin. And the inlet velocity follows a sinusoidal equation.

This will allow the computational software to compute the interactions between the magnetic vector potential generated by the permanent magnet and the magnetic nanoparticles in the blood. These interactions are simulated based on Maxwell equations at the location where the magnetic sensor is placed. The simulated magnetic field at the sensor location is found to assume similar sinusoidal waveform characteristics as the inlet velocity of the blood. The amplitude of the simulated waveforms at the sensor location are compared with physical measurements on human subjects and found to be highly correlated.

***Keywords*—** blood pulse, magnetic sensing, non-invasive measurement, magnetic disturbance

I. Introduction

WITH the advancement of bioelectronics, portable health monitoring devices are getting popular because they are able to provide continuous monitoring of an individual's health condition with ease of use and comfort. Robust and portable health monitoring devices are increasingly required at places such as home, ambulance and hospital, and at situations including military training and sports.

Pulse rate is a measurement of the number of times the heart beats per minute. The heart pushes blood through the arteries, which expand and contract allowing blood to flow.

Current methods of heart or pulse rate acquisition can be classified into electrical [1][2], optical[3][7], microwave [4], acoustic [5][8][11], mechanical [6][9] or magnetic [10][12][13] means. Each of these methods has been studied in detail and its limitations have been well published and known.

The method of study here involves a simple and yet reliable magnetic means to acquire blood pulse [15]. Such a method measures the magnetic disturbance created by blood (i.e. Modulated magnetic signature of blood - MMSB) in a constant magnetic flux and will support the acquisition of blood pulse without the need for a good electrical or optical contact. Therefore, this method can be used to acquire pulse rate over a prolonged period of time.

In order to model MMSB, the flow of a biomagnetic fluid (i.e. blood) in a weak magnetic field strength (0.1-0.2 Tesla) will be investigated. As such, Biomagnetic fluid dynamics (BFD) by Haik et al [16] will be used, which deals with no induced electric current, and assumes that the flow of blood is affected by its magnetization properties.

II. Simulation Model

A. Model creation

1) Geometry description

The 2-dimensional simulation model geometry represents an oxygenated blood vessel embedded in a thin layer of tissues (skin) with a permanent magnet and magnetic sensor placed in close proximity as illustrated in Fig. 1. The model is created based on the proposed blood pulse measurement method using MMSB as outline in [15]. The domains labeled Air and Tissues in Fig. 1 are modeled as non-magnetic and have dimensions large (i.e. at least 5 times larger) as compared to the critical components in the simulation model (i.e. magnetic sensor, permanent magnet, skin and blood vessel). Therefore, the simulation results will be independent on these domains.

2) Magnetic environment and blood flux equations

The magnetic field sensor is modeled as a passive non-magnetic device capable of translating the magnetic field into potential difference output (i.e. voltage) following a non-linear function as shown in Fig. 2. However, the magnetic field sensor can be biased in this simulation model to operate as a linear sensor with high sensitivity.

The velocity and pressure fields in the blood stream are modeled based on Navier-Stroke equations, describing the time-dependent mass and momentum balances for an incompressible flow. The walls of the blood vessel are

Chee Teck Phua is with the Nanyang Polytechnic of Singapore, 180 Ang Mo Kio Avenue 8 Singapore 569830 (Phone: +65-6550-0703; Fax: +65-6440-0404; e-mail:phua_chee_teck@nyp.gov.sg).

Gaëlle Lissorgues is with ESIEE – ESYCOM , University Paris Est, France (e-mail: lissorguesg@esiee.fr).

assumed to have no-slip condition, u = v = 0 , where u is the fluid velocity and v is the velocity of the wall.

The outlet of the blood vessel is setup as zero pressure and the inlet boundary blood assumes a parabolic flow profile. The normal inflow velocity is accordance to 4 $U_m s(1-s)$, [20] where s is a boundary segment length parameter that goes from 0 to 1 along the inlet boundary segment and U_m is the maximal flow velocity. The inflow velocity is assumed to follow a sinusoidal expression in time as described in (1) to emulate the heart beat.

$$U_0 = 10.U_m.s.(1-s).\{\sin(\omega t) + \sqrt{\sin[(\omega t)^2]}\} \quad (1)$$

With the presence of a permanent magnet in the simulation model, the magnetic part of the model will be static and the Maxwell-Ampere's law for the magnetic field H (A/m) and the current density J (A/m^2) in (2) can be applied. In addition, Gauss' law for the magnetic flux density B (V_s/m^2) is stated in (3). This will result in the constitutive equations describing the relationships between B and H in the different parts of the modeling domain as shown in (4).

$$\nabla \times H = J \quad (2)$$

$$\nabla \times B = 0 \quad (3)$$

$$B = \begin{cases} \mu_o \mu_{r,mag} H + B_{rem} & permanent\ magnet \\ \mu_0 \left(H + M_{ff}(H)\right) & blood\ stream \\ \mu_0 H & tissue\ and\ air \end{cases} \quad (4)$$

μ_0 is the magnetic permeability of vacuum ($V_s/(A \cdot m)$)
$\mu_{r,mag}$ is the relative magnetic permeability of the permanent magnet
$\mathbf{B}_{rem}$ is the remanent magnetic flux (A/m)
$\mathbf{M}_{ff}$ is the magnetization vector in the blood stream (A/m)

Defining a magnetic vector potential A such that B = ∇xA, A = 0 and substituting this into (1) through (3), the equations can be simplified to a 2D problem with no perpendicular currents as shown in (5).

$$\nabla \times \left(\frac{1}{\mu_0} \nabla \times A - M_{ff}\right) = 0 \quad (5)$$

Coupling the magnetic equations with the 2-D model as shown in Fig. 1, the magnetic field at the sensor location will be solved and translated to voltage output using sensor response characteristics as shown Fig. 2.

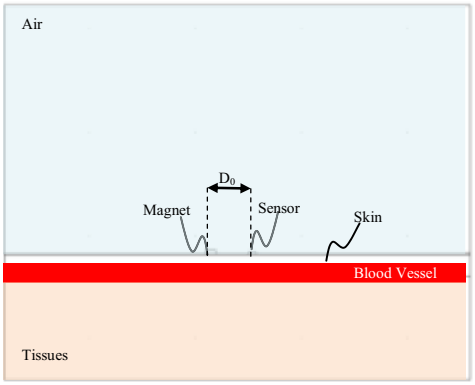

Fig. 1 Illustration of the 2-dimensional simulation model geometry

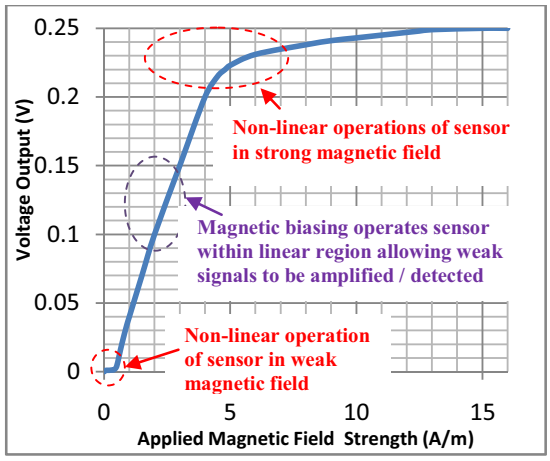

Fig. 2 Non-linear response of sensor with magnetic biasing to achieve linear operations

B. Model parameters and setup

The model developed with COMSOL is setup with the parameters listed in Table 1 and Table 2, where the biomagnetic fluid, blood, is assumed to behave as a magnetic fluid with magnetic property affected by factors such as the state of oxygenation [17]. It is reported that blood possesses the property of diamagnetic material when oxygenated and paramagnetic when deoxygenated [18]. Measurements had been performed for the estimation of the magnetic susceptibility of blood which was found to be 3.5×10^{-6} and -6.6×10^{-7} for the venous and arterial blood, respectively [16][19]. In addition, it was reported in [14] that Newtonian reference viscosity $\mu_\infty = 0.00345$ N·s/m^2 and blood density $\rho = 1050$ kg/m^3.

The permanent magnet is modeled based on the physical magnet that is used during experimental. The magnetic flux density is 0.2 Tesla; relative permeability $\mu_{r,mag}$ is 5×10^3; and dimensions of 5 mm diameter and 2 mm height.

The layer of skin between the blood vessel, magnetic and sensor is modeled as a 1 mm layer of non-magnetic tissue. In addition, the layer of tissue below the blood vessel is modeled as a 10 mm layer of non-magnetic tissue.

The layer above the skin is modeled as a layer of air, having 40 mm height, with relative magnetic permeability of 1.

Parameter	Value	Description
mur_mag	5×10^3	Relative permeability, magnet
B_rem	0.2[T]	Remanent flux density, magnet
chi_ff	-0.667×10^{-6}	Magnetic susceptibility, ferrofluid
mur_ff	1+chi_ff	Relative permeability, ferrofluid
k_ff	0.7	Ferrofluid mass fraction in blood stream
Rho	1050[kg/m^3]	Density, blood
μ_∞	0.00345[N·s/m^2]	Newtonian reference viscosity, blood
U_m	50[cm/s]	Maximum flow velocity
F	60[1/min]	Heart-beat rate
Ω	2*pi[rad]*f	Pulse angular velocity

Table 1 Parameters (values) used for simulation model

Name	Expression	Description
Mu0	Mu0_qa	Permeability of vacuum
M_ffx	K_ff*(chi_ff/mu0)*Azy	Induced ferrofluid magnetization, x-component
M_ffy	-k_ff*(chi_ff/mu0)*Azx	Induced ferrofluid magnetization, y-component
F_ffx	k_ff*(Azx*Azxx+Azy*Azxy)* chi_ff/(mu0*(1+chi_ff)^2)	Ferrofluid volume force, x-component
F_ffy	k_ff*(Azx*Azxy+Azy*Azyy)* chi_ff/(mu0*(1+chi_ff)^2)	Ferrofluid volume force, y-component

Table 2 Parameters (expressions) used for simulation model

The model is simulated by varying the distance between the sensor and the magnet, D_0. The amplitude obtained for each simulation will be used for comparison with experimental measurements in the Section III.

C. *Numerical solutions*

The model is verified to be properly setup by comparing first the simulated waveform at the sensor, which has an amplifier gain of 100 (Fig. 4), with the input sinusoidal (1) (Fig. 3). Based on these two plots, it can be concluded that the model is able to simulate the MMSB phenomena.

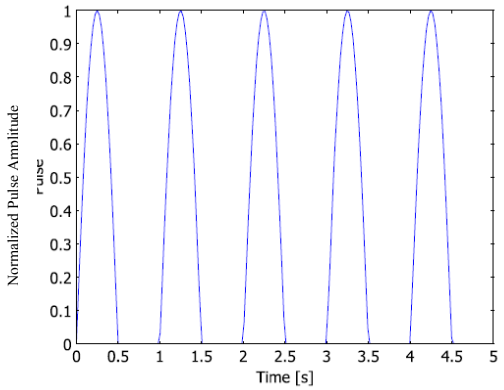

Fig. 3 Input sinusoidal emulating the heart beat

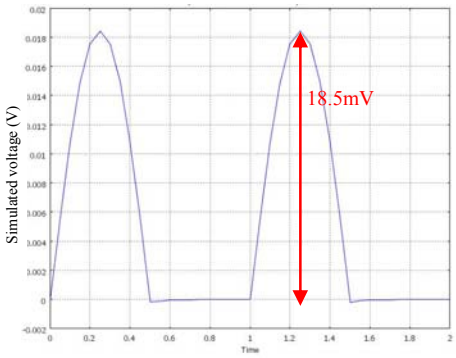

Fig. 4 Simulation results for 2 seconds based on a distance of 20 mm between magnet and sensor

To compare the simulated results with the MMSB as described in [15], the simulation output (Fig. 4) is compared with the ventricular response of the measured waveform (Fig. 5). From these waveforms, it can be observed that both plots have similar ventricular response with peak voltage of approximately 19mV and total pulse duration of 0.5s.

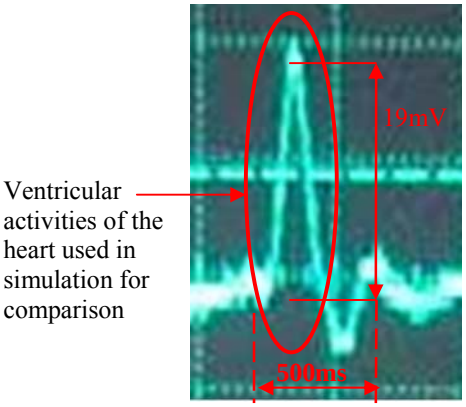

Fig. 5 Waveform captured from the sensor output using oscilloscope for comparison with simulation [15]

With the model verified to be able to simulate MMSB, the distance between the sensor and the magnet, D_0, is varied and plotted with the normalized voltage output as shown in Fig. 6.

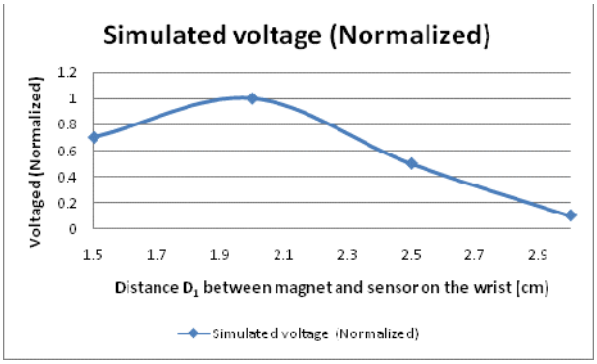

Fig. 6 Plot of simulation results with varying distance between sensor and magnet

III. Comparison with Physical Measurements

A. *Measurement setup*

The experimental measurements on the wrist is setup as shown in Fig. 7. The distance, D_1, between the sensor and the magnet is varied for comparison with the simulation model described in Section II.

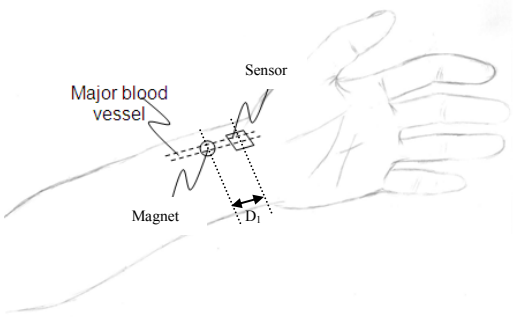

Fig. 7 Illustration of experimental setup for measurement of MMSB on wrist

B. *Measurement results and comparison with the model*

The distance D_1 is varied from 1.5 cm to 3.0 cm and the voltage outputs from the sensor based on multiple measurements are normalized and plotted as shown in Fig. 8. In addition, the average voltage obtained for each D_1 is normalized and plotted in Fig. 9 for comparison with the simulated results as shown in Fig. 6.

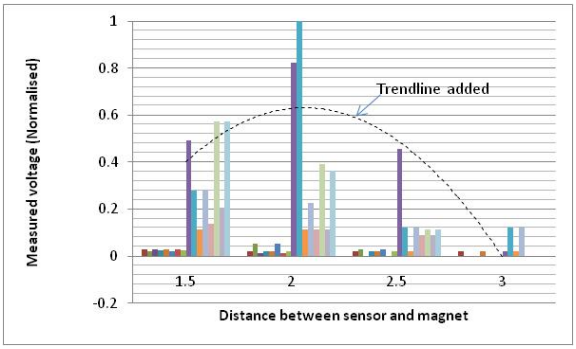

Fig. 8 Plot of voltage (normalized) with varying distance between sensor and magnet

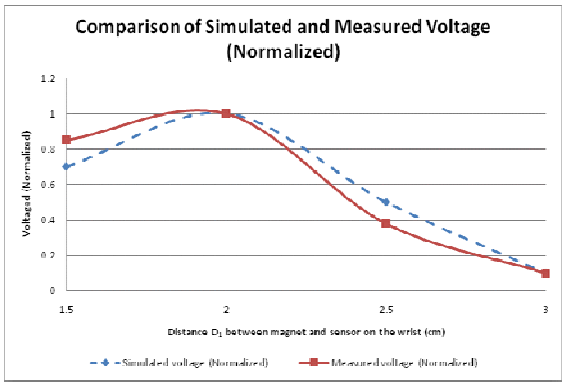

Fig. 9 Plot of average voltage (normalized) with varying distance between sensor and magnet

From Fig. 9, it can be observed that the simulated and measured data both peak at an approximate distance of 2 cm between the sensor and the magnet. In addition, both the simulated and measured voltages decline at a similar rate with respect to distance between the sensor and the magnet.

IV. Conclusion

The simulation model presented in this paper is based on the MMSB phenomena presented in [15]. The simulation model is found to be highly correlated with experimental results and it can be concluded that the simulation model has successfully modeled the MMSB phenomena. Such a model will allow design optimization of MMSB for physical implementation of a wearable device for pulse rate measurements.

With the completion of MMSB modeling in a simulation environment, future work will focus on the applications of MMSB for blood flow analysis.

Acknowledgment

The authors would like to thank Nanyang Polytechnic of Singapore and ESIEE, France for the opportunity to work on this development. In particular, the authors would like to express their gratitude to the School of Engineering (Electronics), Nanyang Polytechnic (Singapore) for the usage of facilities that supported this work.

References

[1] Akinori Ueno, Yasunao Akabane, Tsuyoshi Kato, Hiroshi Hoshino, Sachiyo Kataoka, Yoji Ishiyama (2007), "Capacitive Sensing of Electrocardiographic Potential Through Cloth from the Dorsal Surface of the Body in a Supine Position: A Preliminary Study", IEEE Transactions on Biomedical Engineering, Vol. 54, No. 4, April

[2] S. Bowbrick, A. N. Borg. Edinburgh (2006), "ECG complete", New York, Churchill Livingstone

[3] S. M. Burns (2006), "AACN protocols for practice: noninvasive monitoring", Jones and Bartlett Publishers

[4] Shuhei Yamada, Mingqi Chen, Victor Lubecke (2006), "Sub-uW Signal Power Doppler Radar Heart Rate Detection", Proceedings of Asia-Pacific Microwave Conference

[5] G. Amit, N. Gavriely, J. Lessick, N. Intrator (2005), "Automatic extraction of physiological features from vibro-acoustic heart signals : correlation with echo-doppler", Computers in Cardiology, Issue September 25-28, pp 299-302

[6] J.L. Jacobs, P. Embree, M. Glei, S. Christensen, P.K. Sullivan (2004), "Characterization of a Novel Heart and Respiratory Rate Sensor", Proceedings of the 26th International Conference of the IEEE EMBS

[7] M.N. Ericson, E.L Ibey, G.L. Cote, J.S. Baba, J.B. Dixon (2002), "In vivo application of a minimally invasive oximetry based perfusion sensor", Proceedings of the Second Joint EMBS/BMES Conference

[8] Luis Torres-Pereira, Cala Torres-Pereira, Carlos Couto (1997), "A Non-invasive Telemetric Heart Rate Monitoring System based on Phonocadiography", ISIE'97

[9] J. Kerola, V. Kontra, R. Sepponen (1996), "Non-invasive blood pressure data acquisition employing pulse transit time detection", Engineering in Medicine and Biology, Vol 3, Issue 31 Oct-3 Nov, pp 1308 – 1309

[10] J.Malmivuo, R. Plonsey (1995), "Bioelectromagnetism – Principles and Applications of Bioelectric and Biomagnetic Fields", New-York, Oxford University Press

[11] Yasuaki Noguchi, Hideyuki Mamune, Suguru sugimoto, Jun Yoshida, Hidenori Sasa, Hisaaki Kobayashi, Mitsunao Kobayashi (1994), "Measurement characteristics of the ultrasound heart rate monitor", Engineering in Medicine and Biology Society, Engineering Advances: New Opportunities for Biomedical Engineers. Proceedings of the 16th International Conference of the IEEE Vol. 1, Issue 3-6 Nov Pg 670 - 671

[12] J.R. Singer (1980), "Blood Flow Measurements by NMR of the intact body", IEEE Transactions on Nuclear Science, Vol. NS-27, No. 3

[13] Hiroshi Kanai, Eiki Yamano, Kiyoshi Nakayama, Naoshige Kawamura, Hiroshi Furuhata (1974), "Transcutaneous Blood Flow Measurement by Electromagnetic Induction", IEEE Transaction on Biomedical Engineering, Vol. BME-21, No. 2

[14] Khalil M. Khanafer, Prateek Gadhoke, Ramon Berguer and Joseph L. Bull (2006), "Modeling pulsatile flow in aortic aneurysms: Effect of non-Newtonian properties of blood", Biorheology, 43(5): 661-679

[15] Chee Teck Phua, Gaëlle Lissorgues, Bruno Mercier (2008), "Non-invasive acquisition of Blood Pulse using magnetic disturbance technique", International Conference on BioMedical Engineering (ICBME2008)

[16] Y. Haik, V. Pai, and C. J. Chen (1999), ''Biomagnetic fluid dynamics,'' in Fluid Dynamics at Interfaces, edited by W. Shyy and R. Narayanan Cambridge University Press, Cambridge, pp. 439–452

[17] T. Higashi, A. Yamagishi, T. Takeuchi, N. Kawaguchi, S. Sagawa, S. Onishi, and M. Date (1993), "Orientation of erythrocytes in a strong static magnetic field," J. Blood 82, 1328

[18] L. Pauling, and C. D. Coryell (1936), "The magnetic properties and structure of hemoglobin, oxyhemoglobin and carbonmonoxy hemoglobin," in Proc. Natl. Acad. Sci. U.S.A. 22, 210

[19] M. Motta, Y. Haik, A. Gandhari, and C. J. Chen (1998), "High magnetic field effects on human deoxygenated hemoglobin light absorption," Bioelectrochem. Bioenerg. 47, 297

[20] P.A. Voltairas, D.I. Fotiadis, and L.K. Michalis (2002), "Hydrodynamics of Magnetic Drug Targeting," J. Biomech., vol. 35, pp. 813–821.